Strongly correlated states of a small cold-atom cloud from geometric gauge fields

B. Juliá-Díaz,[1,3] D. Dagnino,[1] K. J. Günter,[2] T. Graß,[3] N. Barberán,[1] M. Lewenstein,[3,4] and J. Dalibard[2]

[1]*Dept. ECM, Facultat de Física, U. Barcelona, E-08028 Barcelona, Spain*
[2]*Laboratoire Kastler Brossel, CNRS, UPMC, Ecole Normale Supérieure, 24 rue Lhomond, F-75005 Paris, France*
[3]*ICFO-Institut de Ciències Fotòniques, Parc Mediterrani de la Tecnologia, E-08860 Barcelona, Spain*
[4]*ICREA-Institució Catalana de Recerca i Estudis Avançats, E-08010 Barcelona, Spain*

Using exact diagonalization for a small system of cold bosonic atoms, we analyze the emergence of strongly correlated states in the presence of an artificial magnetic field. This gauge field is generated by a laser beam that couples two internal atomic states, and it is related to Berry's geometrical phase that emerges when an atom follows adiabatically one of the two eigenstates of the atom-laser coupling. Our approach allows us to go beyond the adiabatic approximation, and to characterize the generalized Laughlin wave functions that appear in the strong magnetic-field limit.

PACS number(s): 03.75.Lm, 37.10.Vz, 03.65.Vf, 73.43.−f

I. INTRODUCTION

Trapped atomic gases provide a unique playground to address many-body quantum physics in a very controlled way [1,2]. Studies of ultracold atoms submitted to artificial gauge fields are particularly interesting in this context, since they establish a link with the physics of the quantum Hall effect. Especially intriguing is the possibility of realizing strongly correlated states of the gas, such as an atomic analog of the celebrated Laughlin state [3].

One way to simulate orbital magnetism is to rotate the trapped gas [3,4]. One uses in this case the analogy between the Coriolis force that appears in the rotating frame and the Lorentz force acting on a charged particle in a magnetic field. This technique allows one to nucleate vortices and observe their ordering in an Abrikosov lattice [4]. Another promising method takes advantage of Berry's geometrical phase that appears when a moving atom with multiple internal levels follows adiabatically a nontrivial linear combination of these levels [5]. This can be achieved in practice by illuminating the gas with laser beams that induce a spatially varying coupling between atomic internal levels [6] (for a review of recent proposals, see, e.g. [7]). Recently, spectacular experimental progress has been made with this technique, leading here also to the observation of quantized vortices [8].

In this paper, we focus on the generation of strongly correlated states of the atomic gas with geometrical gauge fields. We show how Laughlin-type states emerge in a small quasi-two-dimensional system of trapped bosonic atoms when two internal states are coupled by a spatially varying laser field. The key point of our approach is to go beyond the adiabatic approximation and study how the possibility of transitions between the internal states modifies the external ground state of the gas. We perform exact diagonalization for $N = 4$ particles, in order to analyze the overlap between the exact ground state of the system and the Laughlin wave function, as a function of the strength of the atom-laser coupling. We identify a region of parameter space in which the ground state, despite having a small overlap with the exact Laughlin state, has an interaction energy close to zero, a large angular momentum, and a large entropy. We show that it can be represented as a Laughlin-like state with a modified Jastrow factor.

To better frame our work, let us first emphasize that it is well known that the adiabatic accumulation of Berry phase induces artificial gauge fields in electroneutral quantum systems [5,9]. These artificial gauge fields of geometric origin are nowadays considered as an important new framework in which strongly correlated quantum states related to fractional quantum Hall physics can be engineered in systems of ultracold atoms [7]. The major contribution of the present paper is to go beyond adiabaticity to show that the main fingerprints of the strongly correlated quantum state are preserved in a significantly broad region of the experimental parameter space, as demonstrated by detailed numerical calculations. This objective is discussed in detail in the framework of the physics of few-body systems, independent of their attainability in the thermodynamic limit, which is beyond the scope of the present paper. This goal is already a realistic one, as there are nowadays a number of experimental groups able to deal with small bosonic clouds using several techniques [10,11]. These experimental developments have triggered a number of theoretical proposals focusing on the production of strongly correlated quantum states in small atomic clouds [12–14].

The paper is organized in the following way. First, in Sec. II, we present the scheme used to generate the artificial gauge field together with the formalism employed. In Sec. III, we present our results, discussing in detail the properties of the Laughlin-like strongly correlated states appearing for different values of the external control parameters. In Sec. IV, we study the analytical representation of the ground state in the strongly correlated Laughlin-like region. Finally, in Sec. V, we provide some conclusions that can be extracted from our work.

II. THEORETICAL MODEL

We consider a small quasi-two-dimensional ensemble of harmonically trapped bosonic atoms in the *x*-*y* plane interacting with a single laser field treated in a classical way. The single-particle Hamiltonian is given by

$$\hat{H}_{\rm sp} = \frac{\boldsymbol{p}^2}{2M} + V(\boldsymbol{r}) + \hat{H}_{\rm AL}, \qquad (1)$$

where M is the atomic mass and $V(\boldsymbol{r})$ is an external potential confining the atoms in the plane. $\hat{H}_{\rm AL}$ includes the atom-laser
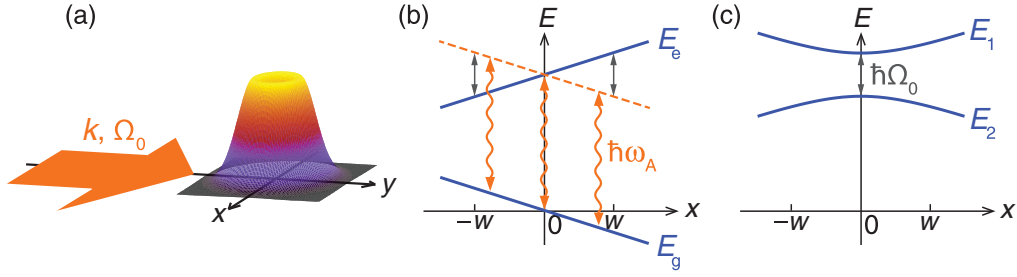
FIG. 1. (Color online) Schematic illustration of the considered setup. (a) Atoms are trapped in the x-y plane and illuminated with a plane wave propagating along the y direction. (b) The energy difference between the two internal states that are coupled by the laser field varies linearly along the x direction. (c) Energy eigenvalues of the atom-laser coupling in the rotating wave approximation.

coupling as well as the internal energies. In order to minimize the technical aspects of the proposal, we consider here a very simple laser configuration to generate the geometrical gauge field. However, it is straightforward to generalize our method to more complex situations. The laser field is a plane wave with wave number k and frequency ω_L propagating along the direction y [see Fig. 1(a)]. It couples two internal atomic states $|g\rangle$ and $|e\rangle$ with a strength that is given by the Rabi frequency Ω_0.

The atom-laser term comes from the coupling of the electric dipole of the atom with the electric field of the laser. It can be written as

$$\hat{H}_{AL} = E_g |g\rangle\langle g| + E_e |e\rangle\langle e| \\ + \hbar\Omega_0 \cos(\omega_L t - \phi)(|e\rangle\langle g| + |g\rangle\langle e|), \quad (2)$$

with $\phi = ky$. We neglect the spontaneous emission rate of photons from the excited state $|e\rangle$, which is a realistic assumption if the intercombination line of alkali-earth or ytterbium atoms is used. For instance, for ytterbium atoms, the state $|e\rangle$ could be taken as the first excited level $6\,^3P_0$ which has a very long lifetime of ~ 10 s [15]. Importantly, we further assume that the energies $E_g = -\hbar\Omega_0 x/(2w)$ and $E_e = \hbar\omega_A + \hbar\Omega_0 x/(2w)$ of the uncoupled internal states vary linearly along x in a length scale set by the parameter w, as sketched in Fig. 1(b). This can be achieved experimentally either by profiting the Zeeman effect, i.e., applying a real magnetic-field gradient to the system, or by using the ac Stark shift produced by an extra laser beam with an intensity gradient. We suppose that the laser is resonant with the atoms in $x = 0$, i.e., $\omega_L = \omega_A$. Using the rotating-wave approximation, $\hat{H}_{AL}$ can be written in the frame rotating with the laser frequency ω_L and in the $\{|e\rangle, |g\rangle\}$ basis [16] as

$$\hat{H}_{AL} = \frac{\hbar\Omega}{2}\begin{pmatrix} \cos\theta & e^{i\phi}\sin\theta \\ e^{-i\phi}\sin\theta & -\cos\theta \end{pmatrix}, \quad (3)$$

where $\Omega = \Omega_0\sqrt{1+x^2/w^2}$, and $\tan\theta = w/x$.

It is convenient to rewrite Eq. (1) in the basis of the local eigenvectors of $\hat{H}_{AL}$, $|\psi_1\rangle_\mathbf{r}$, and $|\psi_2\rangle_\mathbf{r}$, associated to the eigenvalues $\hbar\Omega/2$ and $-\hbar\Omega/2$, respectively. These can

be written in the $\{|e\rangle, |g\rangle\}$ basis as

$$|\psi_1\rangle_\mathbf{r} = e^{-iG}\begin{pmatrix} \cos\theta/2 & e^{i\phi/2} \\ \sin\theta/2 & e^{-i\phi/2} \end{pmatrix},$$

$$|\psi_2\rangle_\mathbf{r} = e^{iG}\begin{pmatrix} -\sin\theta/2 & e^{i\phi/2} \\ \cos\theta/2 & e^{-i\phi/2} \end{pmatrix}, \quad (4)$$

where $G = \frac{kxy}{4w}$. This particular form of Eq. (4) allows us in what follows to obtain a fully symmetric H_{22}; see Eq. (13). Let us emphasize that the choice of the phase factor in front of these eigenstates is nothing but a gauge choice for the following.

The atomic state can be then expressed as

$$\chi(\mathbf{r},t) = a_1(\mathbf{r},t) \otimes |\psi_1\rangle_\mathbf{r} + a_2(\mathbf{r},t) \otimes |\psi_2\rangle_\mathbf{r}, \quad (5)$$

where a_i captures the dynamics of the center of mass and $|\psi_i\rangle_\mathbf{r}$ of the internal degree of freedom (in the following, we drop the subindex $\mathbf{r}$ in the kets $|\psi_{1,2}\rangle$ to simplify the notation). Projecting onto the basis $\{|\psi_i\rangle\}$, and noting that

$$\nabla_\mathbf{r}(a_j\psi_j) = a_j(\nabla_\mathbf{r}\psi_j) + (\nabla_\mathbf{r}a_j)\psi_j, \quad (6)$$

the single-particle Hamiltonian, Eq. (1), is represented by the 2×2 matrix $\hat{H}_{sp} = [H_{ij}]$ acting on the spinor $[a_1(\mathbf{r},t), a_2(\mathbf{r},t)]$. We find, in particular [17,18],

$$H_{jj} = \frac{[\mathbf{p} - \epsilon_j \mathbf{A}]^2}{2M} + U + V + \epsilon_j \frac{\hbar\Omega}{2}, \quad (7)$$

with $\epsilon_1 = 1$ and $\epsilon_2 = -1$, where we have defined

$$\mathbf{A}(\mathbf{r}) = -i\hbar\langle\psi_2|\nabla_\mathbf{r}\psi_2\rangle \quad (8)$$

and

$$U(\mathbf{r}) = \frac{\hbar^2}{2M}[\langle\nabla_\mathbf{r}\psi_2|\nabla_\mathbf{r}\psi_2\rangle + (\langle\psi_2|\nabla_\mathbf{r}\psi_2\rangle)^2]. \quad (9)$$

For the chosen gauge, they read

$$\mathbf{A}(\mathbf{r}) = \hbar k\left[\frac{y}{4w}, \frac{x}{4w} - \frac{x}{2\sqrt{x^2+w^2}}\right], \quad (10)$$

$$U(\mathbf{r}) = \frac{\hbar^2 w^2}{8M(x^2+w^2)}\left(k^2 + \frac{1}{x^2+w^2}\right). \quad (11)$$

We consider atomic clouds extending over distances smaller than w. This allows us to expand the matrix elements H_{ij} up to second order in x and y. In this approximation, we recover the symmetric gauge expression $\mathbf{A}(\mathbf{r}) = \frac{\hbar k}{4w}(y, -x)$ and the artificial magnetic field reduces to $\mathbf{B}_j = [\epsilon_j \hbar k/(2w)]\hat{\mathbf{z}}$ for an

atom in $|\psi_j\rangle$. The specific choice of the phase factors in Eq. (4) is in fact obtained by imposing as a constraint the symmetric gauge at this step. Finally, we fix the external potential $V(\boldsymbol{r})$ such that the total confinement for the spinor component a_2 is isotropic with frequency $\omega_\perp$:

$$\frac{1}{2}m\omega_\perp^2(x^2 + y^2) = U(\boldsymbol{r}) + V(\boldsymbol{r}) - \frac{\hbar\Omega(\boldsymbol{r})}{2} + \frac{A^2(\boldsymbol{r})}{2M}. \quad (12)$$

The Hamiltonian

$$\begin{aligned}
H_{22} &= p^2/2M + \boldsymbol{p}\cdot\boldsymbol{A}/M + M\omega_\perp^2 r^2/2 \\
&= \frac{(\boldsymbol{p}+\boldsymbol{A})^2}{2M} + \frac{M\omega_\perp^2}{2}(1-\eta^2)r^2 \quad (13)
\end{aligned}$$

is thus circularly symmetric and its eigenfunctions are the Fock-Darwin (FD) functions $\phi_{\ell,n}$, with ℓ and n denoting the single-particle angular momentum and the Landau level, respectively. The magnetic-field strength is characterized by $\eta \equiv \omega_c/2\omega_\perp$, with $\omega_c = |B_j|/M = \hbar k/(2Mw)$ the "cyclotron frequency."

The interesting regime for addressing quantum Hall physics corresponds to quasiflat Landau levels, which occur when the magnetic-field strength η is comparable to 1. The energies of the states of the lowest Landau level (LLL), $n = 0$, are $E_{\ell,0} = \hbar\omega_\perp[1 + \ell(1-\eta) + (k^2\lambda_\perp^2/8) + \lambda_\perp^2/(8w^2)]$, where $\lambda_\perp = \sqrt{\hbar/M\omega_\perp}$.

Relevant energy scales of the single-particle problem are $\hbar\Omega_0$, which characterizes the internal atomic dynamics, and the recoil energy $E_R = \hbar^2k^2/(2M)$, which gives the scale for the kinetic energy of the atomic center-of-mass motion when it absorbs or emits a single photon. For $\hbar\Omega_0 \gg E_R$, the adiabatic approximation holds and the atoms initially prepared in the internal state $|\psi_2\rangle$ will remain in this state in the course of their evolution [7]. The single-particle Hamiltonian H_{22}, in combination with repulsive contact interactions, then leads to quantum Hall-like physics, which has already been extensively studied [3]. Our goal here is to consider corrections to the adiabatic approximation and to analyze in which respect these corrections still allow one to reach strongly correlated states. This aspect is particularly important from an experimental point of view, since the accessible range of Ω_0 is limited if one wants to avoid undesired excitation of atoms in the sample to higher levels and/or an unwanted laser assisted modification of the atom-atom interaction. Note that the strength of the atom-laser coupling, characterized by Ω_0, is distinct from the strength of the magnetic field, characterized by η. Because the magnetic field has a geometric origin, η is independent of the atom-laser coupling as long as the adiabatic approximation is meaningful.

In the following, we consider the situation where $\hbar\Omega_0$ is still relatively large compared to E_R, so that we can treat the coupling between the internal subspaces related to $|\psi_{1,2}\rangle$ in a perturbative manner. In a systematic expansion in powers of Ω_0^{-1}, the first correction to the adiabatic approximation consists (for the spinor component a_2) of replacing H_{22} by the effective Hamiltonian [16]

$$H_{22}^{\text{eff}} = H_{22} - \frac{H_{21}H_{12}}{\hbar\Omega_0}. \quad (14)$$

The additional term $H_{21}H_{12}/(\hbar\Omega_0)$, which does not commute with the total angular momentum, is somewhat reminiscent

of the anisotropic potential that is applied to set an atomic cloud in rotation [19,20]. It is, however, mathematically more involved and physically richer, as it includes not only powers of x and y, but also spatial derivatives with respect to these variables; see the Appendix for its explicit form.

III. GROUND-STATE PROPERTIES

The quasidegeneracy in the LLL can lead to strong correlations as the interaction picks a many-body ground state for the system. The interaction between the atoms is well described by a contact interaction with a coupling constant $g = \sqrt{8\pi}(a_s/l)$ for the quasi-two-dimensional confinement. Here, a_s is the s-wave scattering length and l the thickness of the gas in the strongly confined z direction. The many-body Hamiltonian then reads

$$H = \sum_{i=1}^{N} H_{22}^{\text{eff}}(i) + \frac{\hbar^2 g}{M}\sum_{i<j}\delta(\boldsymbol{r}_i - \boldsymbol{r}_j). \quad (15)$$

Using an algorithm for exact diagonalization within the LLL of H_{22}, we have determined the many-body ground state (GS) of the system, providing phase diagrams of several relevant average values characterizing the system in a broad range of laser couplings, Ω_0, and magnetic-field strengths, η. To ensure the validity of the LLL assumption, we demand that the difference in energy between different Landau levels is larger than the kinetic energy of any particle in a FD state inside a Landau level. In addition, in the full many-body problem, the interaction energy per particle is always much smaller than the energy difference between adjacent Landau levels. The main results are summarized in Figs. 2, 3, and 4 and discussed in Secs. III A, III B, and III C, respectively. In Sec. III D, we analyze the internal correlations in the Laughlin state and, in Sec. III E, we address the important problem of the role of excitations in the Laughlin-like region. All the calculations are performed for $N = 4$ atoms, $k = 10/\lambda_\perp$, and $gN = 6$. As the perturbation $H_{21}H_{12}$ breaks the rotational symmetry, we cannot carry out the exact diagonalization by restricting ourselves to a subspace with fixed angular momentum as in standard literature. To achieve convergent numerical results, we need to include a large number of L subspaces, and this number grows as $\hbar\Omega_0/E_R$ is decreased. In all cases, we consider all subspaces with $0 \leqslant L < L_{\max}$, where $L_{\max}$ is chosen to ensure convergency. For definiteness, let us quote the size of the Hilbert spaces considered in our work. For $N = 4$, we require $L_{\max} = 28$ for most of the numerical results reported in the paper, which results in a Hilbert space size of 2157. This rapidly growing size of the Hilbert space as N is increased, together with our explicit interest in providing fine-step phase diagrams varying both parameters η and $\hbar\Omega_0$ in a broad region, makes our full study already computationally very extensive, i.e., the calculations presented in this paper require on the order of two weeks on a single 2 GHz processor.

A. Angular momentum

In Fig. 2, we show the expectation value of the total angular momentum of the GS as a function of η and $\hbar\Omega_0/E_R$. For large Ω_0, we recover the steplike structure that is well
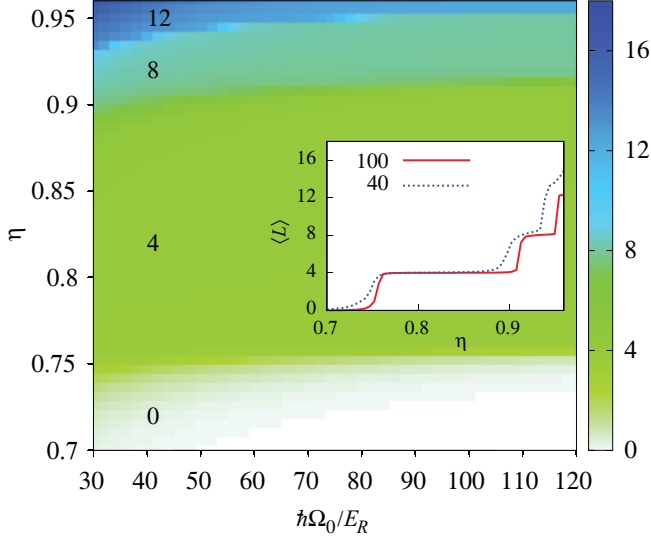
FIG. 2. (Color online) Average value of the total angular momentum, in units of $\hbar$, of the ground state for $N = 4$ atoms as a function of η and $\hbar\Omega_0/E_R$. The insets concentrate on two different values of $\hbar\Omega_0/E_R = 40$ and 100, respectively.

FIG. 3. (Color online) Entropy of the ground state for $N = 4$ atoms as a function of η and $\hbar\Omega_0/E_R$. The insets concentrate on two different values of $\hbar\Omega_0/E_R = 40$ and 100, respectively.

known for rotating bosonic gases, with plateaus at $L = 0, 4, 8$, and 12 [3,21] with $\eta\omega_\perp$ playing the role of the rotating frequency. For an axisymmetric potential containing $N \gg 1$ bosons, it is well known that the value $L = N$ corresponds to a single centered vortex, described by the mean-field state $\Psi_{1vx} = \prod_{i=1}^{N} z_i e^{-\sum z_i^2/2\lambda_\perp}$. Here the squared overlap between our GS and Ψ_{1vx} is relatively low (0.47). This is due to the small value of N, which causes significant deviations from the mean-field prediction. The value $L = N(N-1)$ (here $L = 12$) in the axisymmetric case corresponds to the exact Laughlin state, with a filling factor $1/2$ for any N. For decreasing values of Ω_0, the transitions between the plateaus become broader and are displaced toward smaller values of η. The Laughlin-like region is defined here as the interval of η fulfilling $\langle\mathrm{GS}|\hat{L}|\mathrm{GS}\rangle > N(N-1)$.

B. Entropy

An interesting measure for the correlations in the ground state is provided by the one-body entanglement entropy [22] defined as

$$S = -\mathrm{Tr}[\rho^{(1)} \ln \rho^{(1)}]. \quad (16)$$

Here $\rho^{(1)}$ is the one-body density matrix associated with the GS wave function defined as

$$\rho^{(1)}(\mathbf{r}, \mathbf{r}') = \langle\mathrm{GS}|\hat{\Psi}^\dagger(\mathbf{r})\hat{\Psi}(\mathbf{r}')|\mathrm{GS}\rangle, \quad (17)$$

where $\hat{\Psi}(\vec{r})$ is the field operator, $\hat{\Psi}(\vec{r}) = \sum_\ell \phi_{\ell,0}\hat{a}_{\ell,0}$, with $\hat{a}_{\ell,0}$ the operator that destroys a particle with angular momentum ℓ in the LLL. The natural orbitals, $\phi_i(\mathbf{r})$, and their corresponding occupations, n_i, are defined by the eigenvalue problem,

$$\int d\mathbf{r}\, \rho^{(1)}(\mathbf{r}, \mathbf{r}')\phi_i(\mathbf{r}) = n_i\phi_i(\mathbf{r}'). \quad (18)$$

The entropy of Eq. (16) provides information on the degree of condensation or fragmentation of the system and on the entanglement between one particle and the rest of the system.
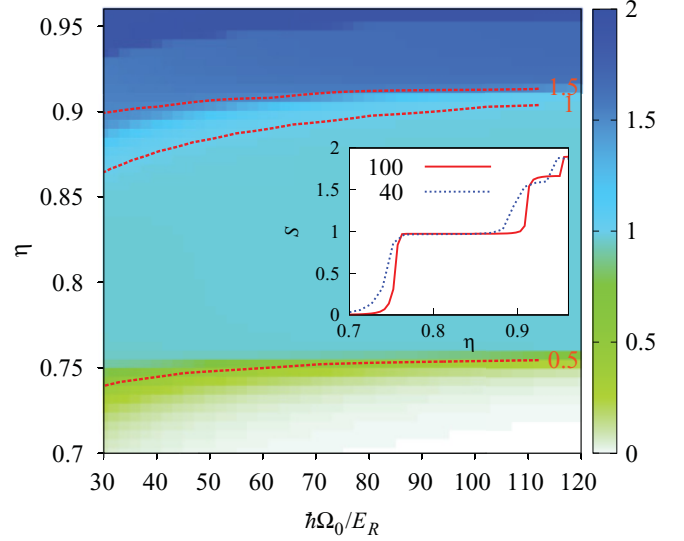
This entropy definition is enough for our characterization of the strong correlations of the ground state. More detailed studies, such as whether our ground state satisfies area laws for the entanglement entropy [23] are beyond the scope of the present paper. The entropy can be explicitly evaluated as $S = -\sum_i n_i \ln n_i$. Thus it can be checked that this entropy is zero for a true Bose-Einstein condensate, since all particles occupy the same mode ($n_1 = 1, n_i = 0, i > 1$). As the system loses condensation, with more than one nonzero eigenvalue, S increases. For the Laughlin wave function with N bosons, $2N - 1$ single-particle states are approximately equally populated, and the entropy is $\sim \ln(2N - 1)$. The entropy S is plotted in Fig. 3 and it presents features that are similar to that of Fig. 2. For a fixed η, the entropy decreases with Ω_0. For fixed Ω_0, the dependence on η exhibits steps, similar to that of $\langle L \rangle$. The region of $\langle L \rangle = 0$ corresponds to a fairly condensed region with $S \sim 0$. In the one vortex region, corresponding to $\langle L \rangle = N$, the condensation is already not complete. This is reflected in the above-mentioned low value of the squared overlap between the GS and Ψ_{1vx}, as well as in the entropy close to 1. Finally, it gradually increases as we increase η, and reaches its maximum value in the Laughlin-like region, $\eta > 0.93$.

C. Interaction energy

In Fig. 4, we depict the average interaction energy as a function of η and $\hbar\Omega_0/E_R$. In the inset, we also plot for $L = 0$ and $L = N = 4$ the analytical result expected in an axisymmetric potential, $E_{\mathrm{int}} = gN(2N - L - 2)/(8\pi)$, valid for $L = 0$ and $2 \leqslant L \leqslant N$ [24]. The interaction energy approaches zero as we increase η, indicating the Laughlin-like nature of the states in the region $\eta \geqslant 0.93$.

The standard bosonic Laughlin state (at half-filling) has the analytical form [25–27]

$$\Psi_{\mathcal{L}}(z_1, \ldots, z_N) = \mathcal{N} \prod_{i<j} (z_i - z_j)^2 e^{-\sum |z_i|^2/2\lambda_\perp^2}, \quad (19)$$
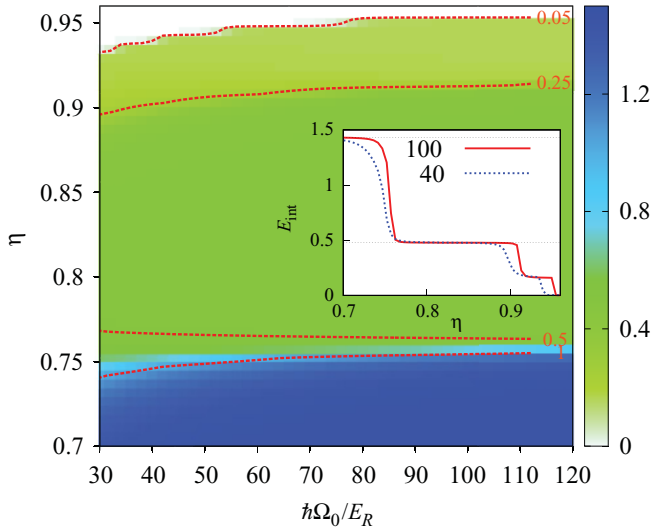
FIG. 4. (Color online) Interaction energy, in units of $\hbar\omega_\perp$, of the ground state for $N = 4$ atoms as a function of η and $\hbar\Omega_0/E_R$. The insets concentrate on two different values of $\hbar\Omega_0/E_R = 40$ and 100, respectively.

where $\mathcal{N}$ is a normalization constant and $z = x + iy$. It is the exact ground state of the system for the contact interaction in the adiabatic case [28]. The contribution of the interaction to the energy of the system is zero due to the zero probability to have two particles at the same place.

D. Internal correlations

The pair correlation function provides a test for the presence of spatial correlations in a system. For the GS, it is defined as

$$\rho^{(2)}(\vec{r}, \vec{r}_0) = \langle GS | \hat{\Psi}^\dagger(\vec{r}) \hat{\Psi}^\dagger(\vec{r}_0) \hat{\Psi}(\vec{r}_0) \hat{\Psi}(\vec{r}) | GS \rangle. \quad (20)$$

In Fig. 5, panels (c) and (d), $\rho^{(2)}(\vec{r}, \vec{r}_0)$ is depicted, where $\vec{r}_0$ is taken as the maximum of the corresponding density, depicted in panels (a) and (b). As seen in the figure, once one particle is detected in $\vec{r}_0$, the other three appear localized at the remaining three vertices of a rectangle. This feature, present also in the exact Laughlin wave function, survives both for $\hbar\Omega_0/E_R = 40$ and 100, even though the squared overlap of the ground state with the Laughlin differs almost by a factor of 2, as will be discussed later in Sec. IV. In the adiabatic case, this spatial correlation could be inferred from the structure of the analytical expression, i.e., the particles tend to avoid each other to minimize energy. This is responsible for the particular spatial correlation shown in panels (c) and (d). No other ground state with $L < N(N-1)$ exhibits this property. A similar phenomenology was found for fermions [29].

E. Energy spectrum

To further characterize the properties of the system, we discuss the properties of the low-energy spectrum and its evolution as we decrease Ω_0, i.e., increasing the nonadiabaticity. In Fig. 6, we show the energy difference between the ground state and the first ten excitations as a function of η. First, let us recall that in the adiabatic case the spectrum of the system has already been studied in the context of rotating atomic
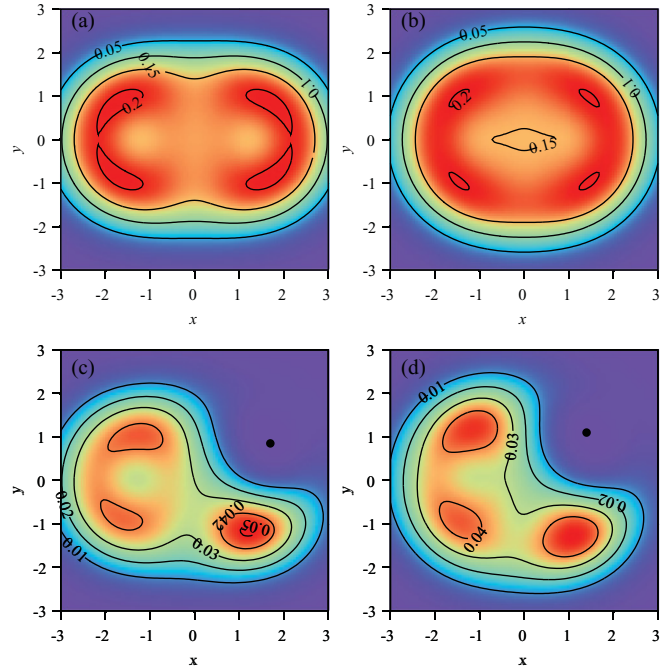

FIG. 5. (Color online) Density of atoms, panels (a) and (b), and pair correlation computed as explained in the text, panels (c) and (d), of the ground state for $\hbar\Omega_0/E_R = 40$ [(a),(c)] and 100 [(b),(d)], respectively. The values of η used are 0.942 and 0.955 for $\hbar\Omega_0/E_R = 40$ and 100, respectively. The solid circle marks the position of $\vec{r}_0$. The length unit is $\lambda_\perp$.

clouds [3]; thus our main interest here will be to characterize the nonadiabatic effects.

Let us first consider the most symmetric case, Fig. 6(b). In the Laughlin region ($\eta > 0.952$), there are two types of lowest excitations: quasiparticle and edge excitations. For $0.952 < \eta < 0.961$, the excitation with $L = N(N-1) - N$ marked as A is a quasiparticle-type state, while for $\eta > 0.961$ the state with $L = N(N-1) + 1$ marked as B_1 is the center of mass excitation. The tower of edge excitations of the system are marked as B_n in the figure and correspond in the adiabatic case to excitations with $L = N(N-1) + n$, with $n > 1$. They are fully degenerate in the adiabatic case with a degeneracy given by the partition function of n, $p(n)$, defined as the number of

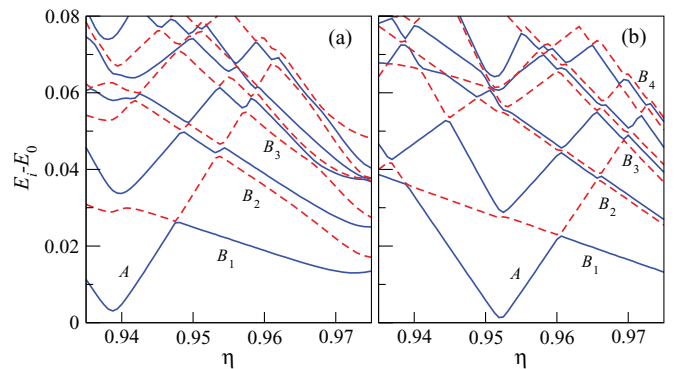

FIG. 6. (Color online) Energy difference in units of $g\hbar\omega_\perp$ between the first 10 levels of the spectrum and the ground-state energy as function of η for $\hbar\Omega_0/E_R = 40$ (a) and 100 (b).

distinct ways in which n can be written as a sum of smaller non-negative integers, i.e., 5 if $n = 4$ [30]. In panel (b), the degeneracy is partly lifted due to the slight nonadiabaticity and in panel (a) the condition is clearly relaxed. This structure of the edge excitations is a fingerprint of the Laughlin state.

Finally, the maximum energy separation between the ground state and its first excitation in the Laughlin region, which in our confined case is both a quasiparticle excitation and the center of mass excitation, increases when decreasing Ω_0. It changes from $\sim 0.022 g\hbar\omega_\perp$ for $\hbar\Omega_0/E_R = 100$ to $\sim 0.027 g\hbar\omega_\perp$ for $\hbar\Omega_0/E_R = 40$. The bulk energy difference in the nonadiabatic cases can be estimated by linearly extrapolating the segment A to $\eta = 1$, giving $\sim 0.18 g\hbar\omega_\perp$ and $\sim 0.13 g\hbar\omega_\perp$ for $\hbar\Omega_0/E_R = 40$ and 100, respectively. Thus, by increasing the laser intensity, the bulk energy difference approaches the value of the gap reported in Ref. [27] for a symmetric and edgeless system.

IV. ANALYTICAL REPRESENTATION OF THE GROUND STATE IN THE LAUGHLIN-LIKE REGION

In this section, we calculate the overlap of the exact solutions for the GS in the Laughlin-like region with several analytical expressions. To begin, we calculate the dependence of the squared overlap $|\langle\Psi_\mathcal{L}|GS\rangle|^2$ of the Laughlin state with the exact GS as a function of the magnetic-field strength η and the atom-laser coupling Ω_0. The result is plotted in Fig. 7. For large Ω_0 (typically $> 80 E_R/\hbar$), the adiabatic approximation holds ($H_{22} \approx H_{22}^{\text{eff}}$): the overlap between the GS and the Laughlin state jumps from a quasizero to a large (> 0.8) value when the magnetic-field strength η reaches a threshold value.

For smaller Ω_0, the overlap is much smaller even for large η (upper left corner of Fig. 7). In this case, the analytical expression must have Jastrow factors that bring the angular momentum around the value $L = N(N-1)$ and that suppress
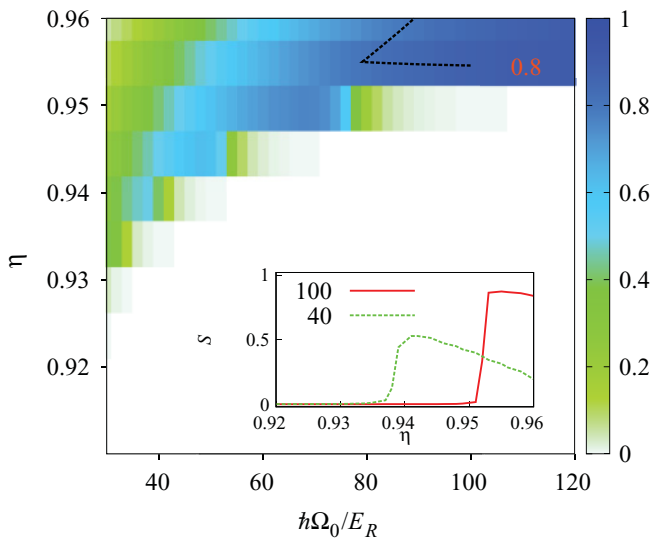

FIG. 7. (Color online) Squared overlap $|\langle GS|\Psi_\mathcal{L}\rangle|^2$ as a function of η and $\hbar\Omega_0/E_R$ for $N = 4$. The dashed line marks the region of squared overlap larger than 0.8. The inset depicts the squared overlap for $\hbar\Omega_0/E_R = 100$ (solid) and 40 (dashed) as a function of η.
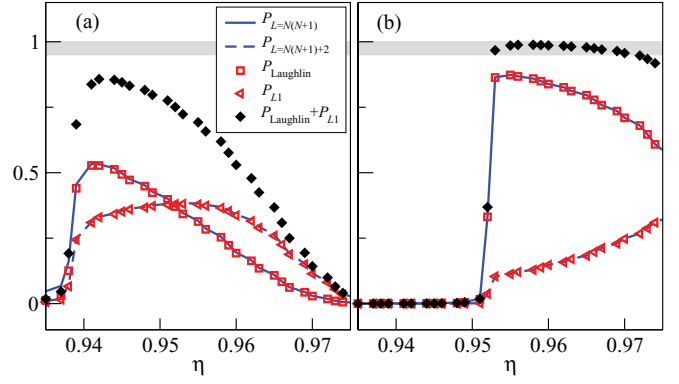

FIG. 8. (Color online) (Upper panels) Squared overlaps between the GS of the system and the Laughlin wave function, $P_{\text{Laug}} = |\langle GS|\Psi_\mathcal{L}\rangle|^2$ (solid squares) and $\Psi_{\mathcal{L}1}$, $P_{L1} = |\langle GS|\Psi_{\mathcal{L}1}\rangle|^2$ (triangles). The sum of both is depicted as solid diamonds. The solid and dashed lines correspond to the weights $P_{L=N(N-1)}$ and $P_{L=N(N-1)+2}$ in the GS, respectively. Panel (a) corresponds to $\hbar\Omega_0/E_R = 40$ and (b) to 100. The shaded band marks the region of squared overlap larger than 0.95. (Lower panels) Energy difference in units of $\hbar\omega_\perp$ between the first 10 levels of the spectrum and the ground-state energy as function of η for $\hbar\Omega_0/E_R = 40$ (c) and 100 (d).

interactions (Figs. 2 and 4). Based on these observations, we propose an analytical ansatz for this GS of the form

$$\Psi_{\mathcal{GL}} = \alpha\Psi_\mathcal{L} + \beta\Psi_{\mathcal{L}1} + \gamma\Psi_{\mathcal{L}2}, \qquad (21)$$

with

$$\Psi_{\mathcal{L}1} = \mathcal{N}_1\Psi_\mathcal{L}\sum_{i=1}^{N}z_i^2,$$

$$\Psi_{\mathcal{L}2} = \mathcal{N}_2(\tilde{\Psi}_{\mathcal{L}2} - \langle\Psi_{\mathcal{L}1}|\tilde{\Psi}_{\mathcal{L}2}\rangle\Psi_{\mathcal{L}1}),$$

$$\tilde{\Psi}_{\mathcal{L}2} = \tilde{\mathcal{N}}_2\Psi_\mathcal{L}\sum_{i<j}^{N}z_iz_j, \qquad (22)$$

such that we ensure $\langle\Psi_\mathcal{L}|\Psi_{\mathcal{L}i}\rangle = 0$ and $\langle\Psi_{\mathcal{L}i}|\Psi_{\mathcal{L}j}\rangle = \delta_{ij}$. This ansatz involves components of angular momentum $L = N(N-1)$ and $L = N(N-1)+2$, and zero interaction energy. The coefficients α, β, and γ are given by the projections of the exact GS onto $\Psi_\mathcal{L}$, $\Psi_{\mathcal{L}1}$, and $\Psi_{\mathcal{L}2}$, respectively. In Figs. 8(a) and 8(b), we present the squared overlaps P_{Laughlin}, P_{L_1} and $P_{\text{Laughlin}} + P_{L_1}$ between the exact GS wave function and the functions $\Psi_\mathcal{L}$, $\Psi_{\mathcal{L}1}$ and $\Psi_{\mathcal{GL}}$ respectively. We restrict our study to the Laughlin region. We also plot the weights of the angular momentum subspaces in the GS: $P_{L=N(N-1)}$ and $P_{L=N(N-1)+2}$.

The first result of our numerical analysis is that $P_{\mathcal{L}_2}$ is negligible (< 0.005) over the whole range of Fig. 8. Then we note that the relations $P_{L=N(N-1)} \approx P_\mathcal{L}$ and $P_{L=N(N-1)+2} \approx P_{\mathcal{L}1}$ hold over this range. This implies that the deviation with respect to the adiabatic approximation mostly increases the weight of the $\Psi_{\mathcal{L}1}$ component in the GS. For small values of $\hbar\Omega_0/E_R$, the squared overlap with the proposed ansatz reaches values of ~ 0.85, with the weight of $\Psi_\mathcal{L}$ and $\Psi_{\mathcal{L}1}$ being of comparable size. As $\hbar\Omega_0/E_R$ increases above 80, the GS is very well represented by Eq. (19), as already explained. Considering different particle numbers from $N = 3$ to $N = 5$,

we always find a very similar behavior and thus conclude that Eq. (21) quite generally provides a good representation of the GS in the Laughlin-like region.[1]

V. SUMMARY AND CONCLUSIONS

In conclusion, we have performed exact diagonalization to analyze the ground state of a small cloud of bosonic atoms subjected to an artificial gauge field. Our approach allowed us to explore both the regime of very large atom-laser coupling, where the adiabatic approximation is valid, and the case of intermediate coupling strengths. In the first case, we recovered the known results for a single component gas in an axisymmetric potential. The second case is crucial for practical implementations because it requires less light intensity on the atoms, which decreases the residual heating due to photon scattering. In this case, we have identified a regime where a strongly correlated ground state emerges, which shares many similarities with the Laughlin state in terms of angular momentum, energy, internal spatial correlations, and lowest excitations, although the overlap between the two remains small. Importantly, a reduction of the laser intensity shifts the region where Laughlin-like states exist to lower values of the effective magnetic field, thus departing from the instability region, $\eta > 1$. We have also proposed an ansatz that represents the ground state quite accurately for a region of the parameter space. Finally, let us emphasize that the properties analyzed in this paper are measurable quantities, as is the case of the expected value of the angular momentum, the pair correlation distribution, and excitation spectrum.

---

[1]Note that the Laughlin-like region decreases notably in size as N is increased.

APPENDIX: EXPLICIT FORM OF THE $H_{21}H_{12}$ TERM

We provide here the explicit expression for the term $H_{21}H_{12}$ appearing in the perturbatively derived Hamiltonian H_{22}^{eff}. As explained in the text, we consider up to quadratic terms in x and y. The explicit expression then reads

$$
\begin{aligned}
H_{21}H_{12} = &\left(\frac{\hbar^4}{4M^2 w^4} - \frac{2x^2\hbar^4}{M^2 w^6} + \frac{k^2 x^2 \hbar^4}{16 M^2 w^4} + \frac{k^4 x^2 \hbar^4}{64 M^2 w^2} \right. \\
&\left. + \frac{ikxy\hbar^4}{4M^2 w^5} + \frac{k^2 y^2 \hbar^4}{64 M^2 w^4} \right) \\
&+ \left(-\frac{ikx\hbar^4}{4M^2 w^3} - \frac{ik^3 x\hbar^4}{8M^2 w} \right) \partial_y \\
&+ \left(\frac{x\hbar^4}{M^2 w^4} - \frac{iky\hbar^4}{8M^2 w^3} \right) \partial_x \\
&+ \left(-\frac{k^2 \hbar^4}{4M^2} + \frac{k^2 x^2 \hbar^4}{4M^2 w^2} \right) \partial_y^2 \\
&+ \left(-\frac{\hbar^4}{4M^2 w^2} + \frac{x^2 \hbar^4}{2M^2 w^4} \right) \partial_x^2 .
\end{aligned}
\tag{A1}
$$

[1] M. Lewenstein, A. Sanpera, V. Ahufinger, B. Damski, A. S. De, and U. Sen, Adv. Phys. **56**, 243 (2007).

[2] I. Bloch, J. Dalibard, and W. Zwerger, Rev. Mod. Phys **80**, 885 (2008).

[3] N. R. Cooper, Adv. Phys. **57**, 539 (2008).

[4] A. L. Fetter, Rev. Mod. Phys. **81**, 647 (2009).

[5] M. V. Berry, Proc. R. Soc. London A **392**, 45 (1984).

[6] R. Dum and M. Olshanii, Phys. Rev. Lett. **76**, 1788 (1996); R. Dum, J. I. Cirac, M. Lewenstein, and P. Zoller, *ibid.* **80**, 2972 (1998).

[7] J. Dalibard, F. Gerbier, G. Juzeliūnas, and P. Öhberg, e-print arXiv:1008.5378 (2010).

[8] Y.-J. Lin, R. L. Compton, K. Jiménez-García, J. V. Porto, and I. B. Spielman, Nature (London) **462**, 628 (2009).

[9] X.-G. Wen, *Quantum Field Theory of Many-Body Systems* (Oxford University Press, New York, 2004).

[10] T. Kinoshita, T. Wenger, and D. S. Weiss, Nature (London) **440**, 900 (2006).

[11] N. Gemelke, E. Sarajlic, and S. Chu, e-print arXiv:1007.2677 (2010).

[12] M. Popp, B. Paredes, and J. I. Cirac, Phys. Rev. A **70**, 053612 (2004).

[13] M. Roncaglia, M. Rizzi, and J. I. Cirac, Phys. Rev. Lett. **104**, 096803 (2010).

[14] M. Roncaglia, M. Rizzi, and J. Dalibard, Sci. Rep. **1**, 43 (2011).

[15] S. G. Porsev, A. Dereviankao, and E. N. Fortson, Phys. Rev. A **69**, 021403 (2004).

[16] C. Cohen-Tannoudji, J. Dupont-Roc, and G. Grynberg, *Atom-Photon Interactions* (Wiley, New York, 1992).

[17] C. A. Mead and D. G. Truhlar, J. Chem. Phys. **70**, 2284 (1979).

[18] M. V. Berry, in *Geometric Phases in Physics*, edited by A. Shapere and F. Wilczek (World Scientific, Singapore, 1989), pp. 7–28.

[19] M. I. Parke, N. K. Wilkin, J. M. F. Gunn, and A. Bourne Phys. Rev. Lett. **101**, 110401 (2008).

[20] D. Dagnino, N. Barberan, M. Lewenstein, and J. Dalibard, Nature Phys. **5**, 431 (2009).

[21] N. Barberán, M. Lewenstein, K. Osterloh, and D. Dagnino, Phys. Rev. A **73**, 063623 (2006).

[22] R. Horodecki, P. Horodecki, M. Horodecki, and K. Horodecki, Rev. Mod. Phys. **81**, 865 (2009).

[23] J. Eisert, M. Cramer, and M. B. Plenio, Rev. Mod. Phys. **82**, 277 (2010).

[24] G. F. Bertsch and T. Papenbrock, Phys. Rev. Lett. **83**, 5412 (1999).

[25] N. R. Cooper, N. K. Wilkin, and J. M. F. Gunn, Phys. Rev. Lett. **87**, 120405 (2001).

[26] R. B. Laughlin, Phys. Rev. Lett. **50**, 1395 (1983).

[27] N. Regnault and T. Jolicoeur, Phys. Rev. Lett. **91**, 030402 (2003).

[28] N. K. Wilkin and J. M. F. Gunn, Phys. Rev. Lett. **84**, 6 (2000).

[29] K. Osterloh, N. Barberan, and M. Lewenstein, Phys. Rev. Lett. **99**, 160403 (2007).

[30] M. A. Cazalilla, Phys. Rev. A **67**, 063613 (2003).